



A dextrorotatory residues-incorporated bioactive dodecapeptide against enterohemorrhagic *Escherichia coli*

Ping Zeng^{1,2}, Xuemei Yang³, Kwok-Yin Wong², Sheng Chen³, Kin-Fai Chan^{2*}, Sharon Shui Yee Leung^{1*}, Lanhua Yi^{4*}

¹School of Pharmacy, Faculty of Medicine, The Chinese University of Hong Kong, Hong Kong 999077, China

²State Key Laboratory of Chemical Biology and Drug Discovery and Department of Applied Biology and Chemical Technology, The Hong Kong Polytechnic University, Hong Kong 999077, China

³Department of Food Science and Nutrition, The Hong Kong Polytechnic University, Hong Kong 999077, China

⁴College of Food Science, Southwest University, Chongqing 400715, China

***Correspondence:** Kin-Fai Chan, State Key Laboratory of Chemical Biology and Drug Discovery and Department of Applied Biology and Chemical Technology, The Hong Kong Polytechnic University, Hung Hom, Kowloon, Hong Kong 999077, China. kf.chan@polyu.edu.hk; Sharon Shui Yee Leung, School of Pharmacy, Faculty of Medicine, The Chinese University of Hong Kong, Shatin, Hong Kong 999077, China. sharon.leung@cuhk.edu.hk; Lanhua Yi, College of Food Science, Southwest University, Chongqing 400715, China. yilanhuaswu@163.com

Academic Editor: Marcello Iriti, Milan State University, Italy

Received: February 22, 2023 **Accepted:** April 23, 2023 **Published:** June 30, 2023

Cite this article: Zeng P, Yang X, Wong KY, Chen S, Chan KF, Leung SSY, et al. A dextrorotatory residues-incorporated bioactive dodecapeptide against enterohemorrhagic *Escherichia coli*. *Explor Drug Sci.* 2023;1:210–20. <https://doi.org/10.37349/eds.2023.00014>

Abstract

Aim: This study aims to report an engineered peptide zp39 with favorable bioactivity against enterohemorrhagic *Escherichia coli* (*E. coli*, EHEC). Its antibacterial mechanisms and application in a real food system are assessed.

Methods: Spatial conformation of synthetic peptide zp39 (GIIAGIIiKIKk-NH₂, lowercase letters indicate dextrorotatory amino acids) was predicted by PEPstrMOD and its secondary structure was further determined by circular dichroism (CD) spectroscopy. Then, standard *E. coli* O157:H7 strain ATCC 43888 was used to evaluate the bioactivity of zp39. A double dilution method was applied to investigate its efficacy in normal broth medium, serum, and highly saline conditions. Its effects on cell membrane permeability and potential were measured by fluorescent assays. Thereafter, morphological changes of *E. coli* O157:H7 cells were monitored by electron microscopy technologies. Finally, the potential application of zp39 in controlling EHEC in food was tested with spinach juice and the *Galleria mellonella* larvae model was employed to assess the *in vivo* efficacy.

Results: Peptide zp39 presented an amphiphilic helical structure. It effectively inhibited the growth of *E. coli* O157:H7 at a concentration of 4 μmol/L in a bactericidal mode. Mechanistic studies revealed that it affected membrane permeability and potential in a dose-dependent manner. Moreover, zp39 maintained satisfactory bioactivity against *E. coli* O157:H7 even in the presence of 70% serum or 1,000 μmol/L chloride salts. In spinach juice application, > 90% *E. coli* O157:H7 cells were killed within 2 h after exposure to



64 $\mu\text{mol/L}$ zp39. *In vivo* study proved that treatment with 64 $\mu\text{mol/L}$ zp39 could effectively boost the survival ratio of infected larvae by 50%.

Conclusions: This study depicts a synthetic dodecapeptide that shows the potential application in controlling EHEC. This molecule may be developed into a highly effective antimicrobial agent applied to prevent food contamination and associated infections.

Keywords

Antimicrobial peptide, dextrorotatory amino acid, *E. coli* O157:H7, membrane damage, spinach juice

Introduction

Enterohemorrhagic *Escherichia coli* (*E. coli*, EHEC) has long been recognized as an important foodborne pathogen [1]. Thereinto, *E. coli* O157:H7 is the most typical serotype, associated with strong toxicity and severe clinical symptoms [2]. EHEC O157:H7 is transmitted to humans primarily through consuming contaminated meat, dairy products, or vegetables because food is one of the most major carriers of this bacteria [3]. A multistate outbreak of *E. coli* O157:H7 in the USA, which led to 116 hospitalized and 5 deaths in 2006, was attributed to bagged spinach [4]. Eleven years later in 2017, another outbreak was found to be associated with *E. coli* O157:H7 contamination in soy nut butter, resulting in 32 cases (> 80% occurred in children) [5]. These incidents suggest the current food safety control strategy may not be sufficient to combat this foodborne pathogen. In this context, developing novel alternatives to control the rapid spread of *E. coli* O157:H7 is highly demanded.

Peptides and their derivatives are a class of antibacterial molecules demonstrating great potential [6]. To date, multiple peptide-based compounds have been used in the fields of medicine and food industry [7]. For instance, glycopeptide vancomycin was applied to treat bacterial infections, especially against Gram-positive strains [8]. Nisin, a naturally isolated cyclic peptide, is the only bacteriocin that was approved to be used as a food additive [9]. Pexiganan, a linear peptide with 22 residues, has achieved commoditization and is employed as a high-efficient template to design novel analogs [10]. Furthermore, the latest advances have shown that antimicrobial peptides could be promising weapons against *E. coli* O157:H7 [11, 12].

Previously, we have reported a linear engineered peptide GIIAGIIKIKK-NH₂ (denoted as zp3) showing potent bioactivity against *E. coli* ATCC 25922 with a minimal inhibitory concentration (MIC) at 8 $\mu\text{mol/L}$ [13]. By substituting isoleucine at position 8 and lysine at position 12 to their corresponding dextrorotatory enantiomers, the new peptide GIIAGIiKIKk-NH₂ (denoted as zp39) has shown better protease stability. In the present study, we investigated its potential application in controlling EHEC O157:H7 which has been proven to cause more damage to the human body than *E. coli* ATCC 25922 [14], offering better clinical insights into its potential application.

Materials and methods

Synthesis and structural characterization of zp39

Peptide zp39 was customized by Synpeptide Co., Ltd (Nanjing, China) with > 90% purity. The structural model of zp39 was predicted by an online website PEPstrMOD (<https://webs.iitd.edu.in/raghava/pepstrmod/>) [15]. The obtained predictive file was visualized by Molsoft interactive PDB fast viewer (<https://molsoft.com/pdbv.html>). Helical wheel projection was generated by NetWheels with a few modifications to highlight the unnatural residues (<http://lbqp.unb.br/NetWheels/>).

For circular dichroism (CD) spectroscopy, zp39 powder was dissolved in water (1 mM). Then, the peptide solution was diluted to 0.05 mM by 10%, 30%, 50%, 70%, and 90% trifluoroethanol (TFE) in water respectively. Spectra were recorded by a J-810 spectrometer (Jasco, Japan). Detailed parameters: room temperature; start wavelength 260 nm; end wavelength 190 nm; data interval 0.1 nm; bandwidth 1 nm; scanning speed 100 nm/min. The original $[\theta]_{\text{obs}}$ was then transferred to $[\theta]$ by the formula: $[\theta] = [\theta]_{\text{obs}}/$

10rlc, where $[\theta]_{\text{obs}}$ is the observed CD values; $[\theta]$ = residue ellipticity; r = amino acid residues (12); l = optical path (1 cm); c = sample concentration (0.05 mM). The helical ratio was roughly calculated by the formula: helical (%) = $(-[\theta]_{222} + 3,000)/39,000$ [16], where $[\theta]_{222}$ is the calculated $[\theta]$ at the wavelength of 222 nm.

MIC

The standard *E. coli* O157:H7 strain, whose identifier is ATCC 43888, was obtained from our in-house bacterial bank [17]. The strain of ATCC 43888 does not produce either Shiga-like toxin I or II and does not possess the genes for these toxins. The MIC value of zp39 was determined following the broth double-dilution method [18]. Briefly, single-colony bacteria grown on Mueller-Hinton agar (MHA, Hopebio, China) was resuspended in Mueller-Hinton broth (MHB, Hopebio, China) to 600 nm optical density (OD_{600}) at 0.1. Next, a total of 5 μL of the bacterial solution was mixed with 150 μL of MHB medium containing various amount of zp39 (0, 2, 4, 8, 16, and 32 $\mu\text{mol/L}$). The OD_{600} values were recorded by a microplate reader (CLARIOstar[®] Plus Microplate Reader, BMG labtech, Germany) after 18 h culture at 37°C. The MIC value was determined as the lowest peptide concentration that resulted in no observed bacterial growth.

Growth curve

E. coli O157:H7 was inoculated into MHB medium, and then mixed with various amount of zp39 (0, 2, 4, 8, 16, and 32 $\mu\text{mol/L}$). The bacterial cells were incubated at 37°C and OD_{600} values were recorded every 2 h for 12 h.

Time-kill curve

The initial cell density of *E. coli* O157:H7 was adjusted to around 10^7 colony forming units (CFU) per milliliter (CFU/mL). Then, bacterial cells were treated with various amount of zp39 (0, 4, 16, and 32 $\mu\text{mol/L}$). At specific intervals (1, 2, 4, and 8 h), a sample of 10 μL aliquot was withdrawn for serial 10-fold dilution. Prepared solutions (10 μL) were dropped on the surface of MHA plates and incubated overnight at 37°C. Subsequently, bacterial colonies (3–30 valid) were counted and the primary CFUs were calculated.

LIVE/DEAD staining

This experiment was performed according to the manual of the LIVE/DEAD[™] BacLight[™] Bacterial Viability Kit (Invitrogen, USA). In brief, logarithmic phase *E. coli* O157:H7 cells were collected by 4,000 rpm centrifugation (Eppendorf 5418, Germany) and resuspended in sterile 0.9% NaCl solution (Dieckmann, Hong Kong). Then, bacterial cells were treated with various amount of zp39 for 4 h. After centrifugation, collection, and resuspension, cells were stained by the dye mixture (prepared as per the specification) for 20 minutes. *E. coli* O157:H7 cells were finally rinsed thrice and pipetted onto a clear microscope coverslip for imaging (Nikon Eclipse Ti2E Live-cell Fluorescence Imaging System, Japan).

Stability

These experiments were performed following the MIC broth double-dilution method [18], except fetal bovine serum (HyClone, USA) or salts (NaCl, CaCl_2 , MgCl_2 , Dieckmann, Hong Kong) were added to the medium. For serum test, MHB mediums were replaced with equivalent volumes of serum (10–70%) for individual groups during incubation. For salt test, extra salts (50–1,000 $\mu\text{mol/L}$) were added to MHB mediums during incubation. After 18 h culture at 37°C, the MIC value was determined as abovementioned protocol.

Cytotoxicity

Cytotoxicity was determined by thiazolyl blue tetrazolium bromide (MTT, BioFroxx, Germany) assay [13]. Briefly, human embryonic kidney cells (HEK293) were treated with zp39 at various concentrations for 24 h. Next, a total of 10 μL MTT solution (5 mg/mL) was used to stain for another 4 h. The precipitates were dissolved in 150 μL dimethylsulfoxide (Dieckmann, Hong Kong). Absorbance values at a wavelength of

570 nm were recorded by a microplate reader (Clariostar, BMG LABTECH, Germany). The group treated with phosphate buffered saline (PBS, Sigma-Aldrich, USA) was set as a control (100% survival).

Membrane permeability

E. coli O157:H7 cells ($OD_{600} = 0.6$) were treated with zp39 (0, 4, 8, 16, and 32 $\mu\text{mol/L}$) for 4 h. Next, SYTOX Green (1 $\mu\text{mol/L}$, ThermoFisher, USA) was applied to stain for 10 minutes at room temperature. Under the excitation wavelength at 488 nm, emission spectrums of each group from 500 nm to 600 nm were recorded (Clariostar, BMG LABTECH, Germany). The maximum fluorescence units can be observed at 523 nm.

Membrane potential

The potentiometric probe 3,3'-dipropylthiadicarbocyanine iodide [DiSC₃(5)], ThermoFisher, USA) was applied to evaluate membrane potential dissipation [19]. Briefly, *E. coli* O157:H7 cells at the logarithmic phase were adjusted to OD_{600} value of 0.2 in PBS. Next, cells were stained by 0.5 $\mu\text{mol/L}$ DiSC₃(5) for 1 h. Then, cells were subjected to the treatment of PBS, valinomycin (1 $\mu\text{mol/L}$), and zp39 (4 $\mu\text{mol/L}$ and 16 $\mu\text{mol/L}$) respectively for 5 minutes. Finally, the fluorescence units were measured using a microplate reader (Clariostar, BMG LABTECH, Germany) with an excitation wavelength of 610 nm and an emission wavelength of 660 nm.

Scanning electron microscopy

E. coli O157:H7 cells ($OD_{600} = 0.6$) were divided into two groups. One was treated with PBS and another was treated with 32 $\mu\text{mol/L}$ zp39 for 2 h. Afterward, cells were collected and fixed with 2.5% glutaraldehyde (Tokyo Chemical Industry, Japan) at 4°C overnight. Then, cells were subjected to a series of gradient dehydration by ethanol (Dieckmann, Hong Kong) solutions (50, 70, 90, and 100%, 10 minutes for each concentration). Finally, the specimens were air-dried, coated with gold, and visualized under the scanning electron microscopy (SEM) apparatus (Tescan VEGA3, Czech).

Scanning transmission electron microscopy

The preparation of *E. coli* O157:H7 cells was the same with SEM till fixed in 2.5% glutaraldehyde. Subsequently, cells were washed with PBS and stained with 2% osmium tetroxide (Sigma-Aldrich, USA). Next, cells were dehydrated with 100% ethanol (Dieckmann, Hong Kong) for 10 minutes. A total of 2 μL solution was added to a copper grid for scanning transmission electron microscopy (STEM) imaging (JEOL JEM-2100F, Japan).

Spinach juice assay

Fresh spinach leaves purchased from a local market were squeezed to get the semisolid mash. The solid precipitate was then removed with filter paper. The remaining spinach juice was sterilized through a 0.22 μm filter. Next, *E. coli* O157:H7 cells were added to tested juice samples with the final concentration of $\sim 10^6$ CFU/mL. Then, spinach juice was divided into four groups and treated with 0, 4, 16, and 64 $\mu\text{mol/L}$ zp39, respectively, for 2 h at 4°C. Finally, a total of 10 μL solution was pipetted on the MHB plate from each group. On the second day, the colony for each plate was counted and the original live bacteria was calculated accordingly. All testing concentrations were performed in quintuplicate.

Larvae test

Spinach juice was prepared as above. *E. coli* O157:H7 cells were added into the juice with the final concentration of $\sim 10^6$ CFU/mL. Then, spinach juice was divided into six groups and five of them were treated with PBS, 4, 16, 64 $\mu\text{mol/L}$ zp39, and 64 $\mu\text{mol/L}$ meropenem respectively, for 2 h at 4°C. Subsequently, a total of 10 μL juice was injected into each larva (10 larvae per group). The survival ratio was monitored for 36 h. The larvae group injected with sterile spinach was set as a negative control and the larvae group injected with PBS-treated *E. coli* O157:H7-contaminated juice was set as a positive control.

Statistical analysis

All experiments were performed in triplicate unless specified. The results were expressed as mean \pm standard error. The normality of data was tested by Shapiro-Wilk test. Levene test was used to check for homogeneity of variances from three or more samples. Difference was analyzed by one-way analysis of variance (ANOVA) and Duncan test. The F -test was used to check for homogeneity of two variances and the Student's t -test was used to check for differences. * represents $P < 0.05$, ** represents $P < 0.01$, *** represents $P < 0.001$, and **** represents $P < 0.0001$.

Results

Structural characterization of zp39

The chemical structure of zp39 is depicted in Figure 1A. Note that two unnatural amino acids, dextrorotatory isoleucine, and dextrorotatory lysine are highlighted in blue. The predicted spatial conformation is shown in Figure 1B. As illustrated in Figure 1C, basic polar residues (lysine) are presented in the pink diamond shape while nonpolar residues (glycine, isoleucine, and alanine) are presented in the green hexagon shape. Two amino acids enclosed by hollow purple squares are dextrorotatory residues. They are linked by gray lines to generate a helical wheel projection.

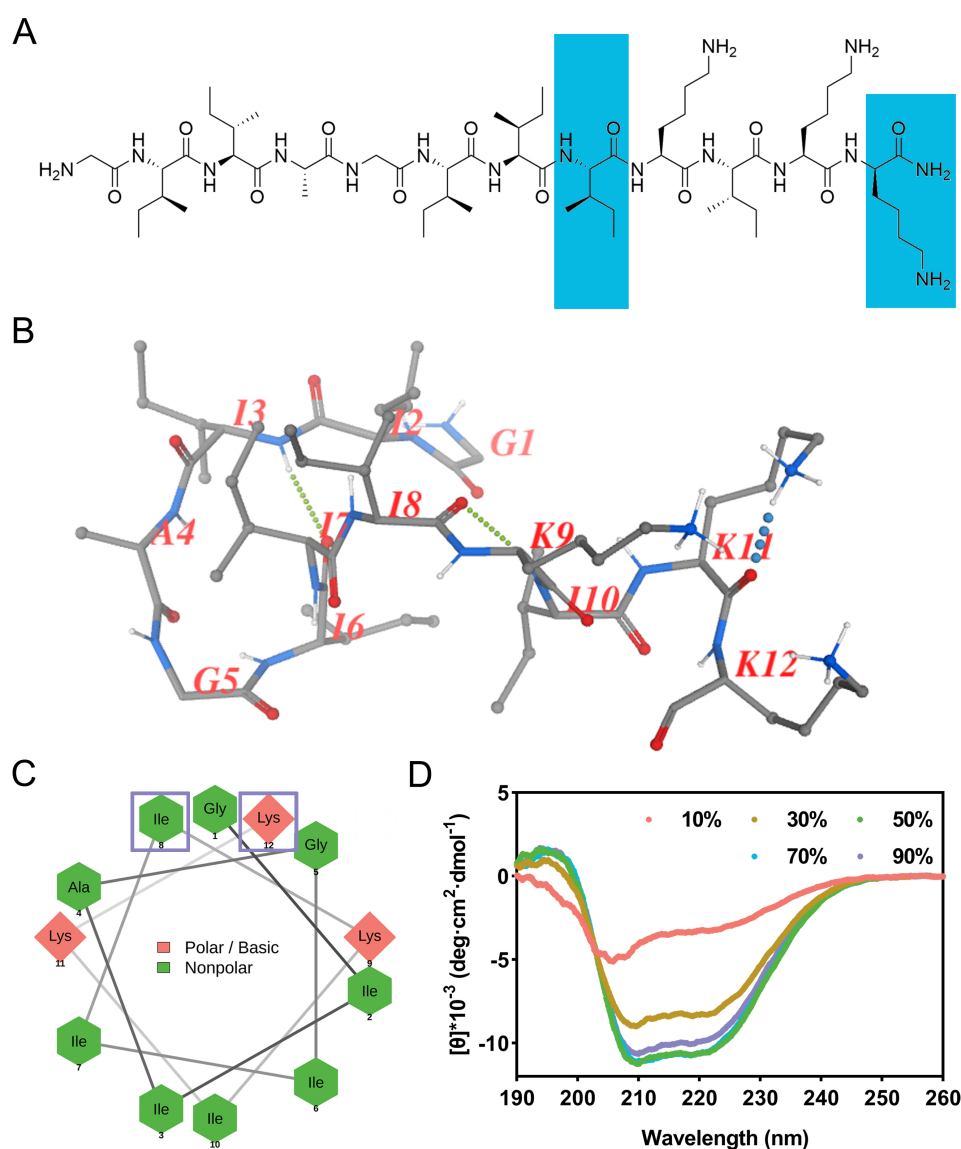


Figure 1. Structural characterization. (A) Chemical structure of zp39 and dextrorotatory residues are highlighted in blue; (B) predicted spatial conformation of zp39; (C) helical wheel projection of zp39 and dextrorotatory residues are enclosed by hollow purple squares; (D) CD spectra of zp39 in different ratio of TFE solutions

In CD spectra (Figure 1D), negative peaks at 208 nm and 222 nm can be detected for all testing conditions. As the ratio of TFE increased from 10% to 50%, the tendency of zp39 to form a helical structure was more obvious. According to the algorithm of beta-structure selection (BeStSel), the helical conformation ratio increased gradually from 4.0% (in 10% TFE) to 24.6% (in 50% TFE). As the proportion of TFE continued to rise, it had little effect on the helical structure. The summary of the proportion of each structure in different concentrations of TFE was shown in Table 1.

Table 1. The proportion of each structure in different concentrations of TFE

TFE (%)	Helix	Antiparallel	Parallel	Turn	Others
10	4.0%	28.9%	2.4%	16.0%	48.7%
30	19.7%	12.5%	7.2%	16.0%	44.6%
50	24.6%	13.2%	7.1%	15.2%	39.8%
70	23.8%	13.1%	7.3%	14.4%	41.4%
90	23.5%	12.6%	7.0%	14.9%	41.9%

Bioactivity of zp39 against *E. coli* O157:H7

Adopting the broth double dilution method, the MIC of zp39 against *E. coli* O157:H7 ATCC 43888 was determined as 4 $\mu\text{mol/L}$. Growth kinetics in the presence of zp39 was monitored in Figure 2A. After 12 h of incubation, no obvious increases in OD_{600} values were detected in testing bacterial samples containing 4, 8, 16, and 32 $\mu\text{mol/L}$ zp39. In contrast, the OD_{600} value of the control group (in the absence of zp39) increased to approximately 1.8. For the 2 $\mu\text{mol/L}$ treatment group, the growth rate comparatively slowed down to a certain extent, but it still reached more than 1.5 in 12 h.

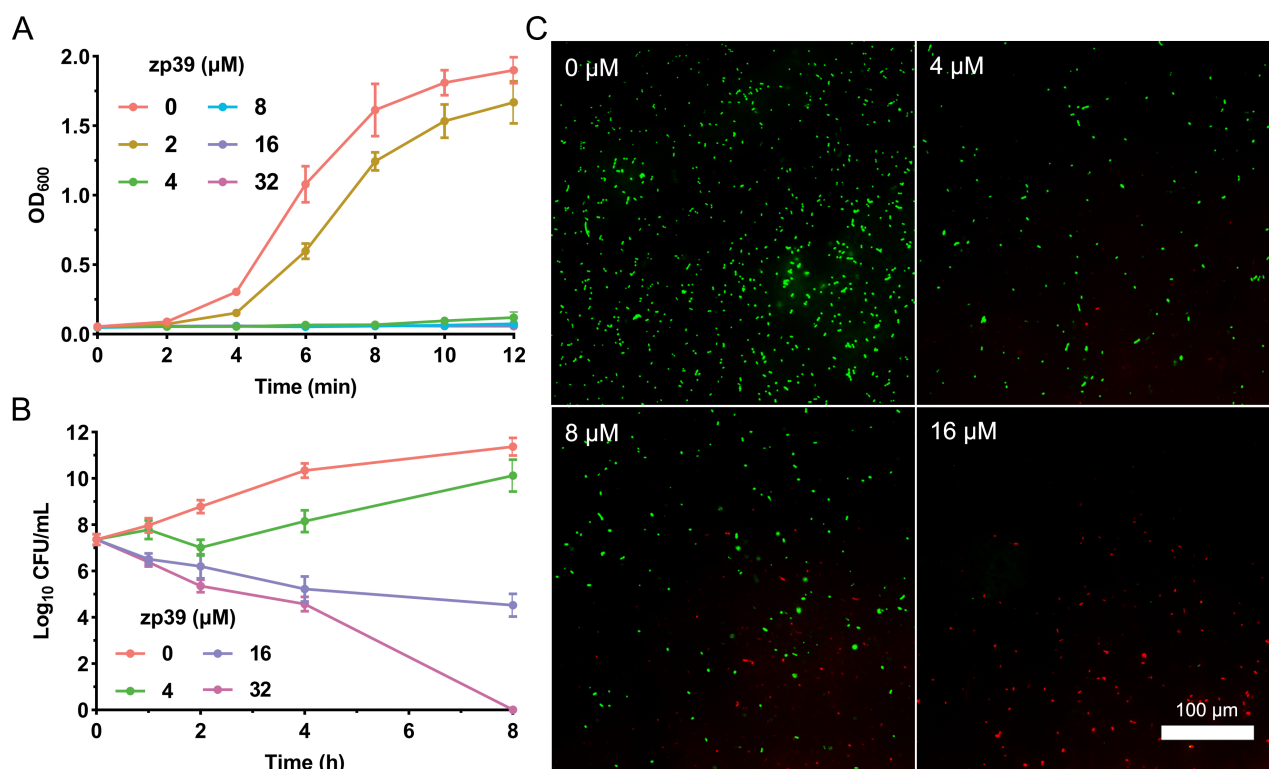


Figure 2. Bioactivity tests of zp39 against *E. coli* O157:H7. (A) Growth curve; (B) time-kill curve; (C) LIVE/DEAD staining

The time-kill curve illustrated in Figure 2B indicated that within 4 h, live colonies of *E. coli* O157:H7 cells decreased from 7.4 \log_{10} CFU/mL to 4.6 \log_{10} CFU/mL in the presence of 32 $\mu\text{mol/L}$ zp39. After 8 h of incubation, the CFU in the highest concentration group was below the lowest detection limit. For other testing groups, live colonies were 11.4 (0 $\mu\text{mol/L}$), 10.1 (4 $\mu\text{mol/L}$), and 4.5 (16 $\mu\text{mol/L}$) \log_{10} CFU/mL respectively.

For LIVE/DEAD staining shown in Figure 2C, *E. coli* O157:H7 cells emitted bright green fluorescence without zp39 treatment. While after incubating with zp39, the green fluorescence gradually decreased and the red fluorescence gradually increased in the visual field in a dose-dependent manner from 0 $\mu\text{mol/L}$ to 4, 8, and 16 $\mu\text{mol/L}$ respectively.

Environmental tolerance and cytotoxicity of zp39

Serum and salt tolerance of zp39 was determined by broth double dilution method. As shown in Figure 3A, in the environment containing serum, the MIC of zp3 and zp39 against *E. coli* O157:H7 gradually increased. In the presence of 60% serum, fold change in MIC of zp3 reached 64 $\mu\text{mol/L}$ and that of zp39 was 16 $\mu\text{mol/L}$. For salt tolerance tests (Figure 3B), even adding extra 1,000 $\mu\text{mol/L}$ chlorides, zp39 remained favorable antibacterial activity against *E. coli* O157:H7 (4, 8, and 16 $\mu\text{mol/L}$ for NaCl, CaCl₂, and MgCl₂ groups, respectively).

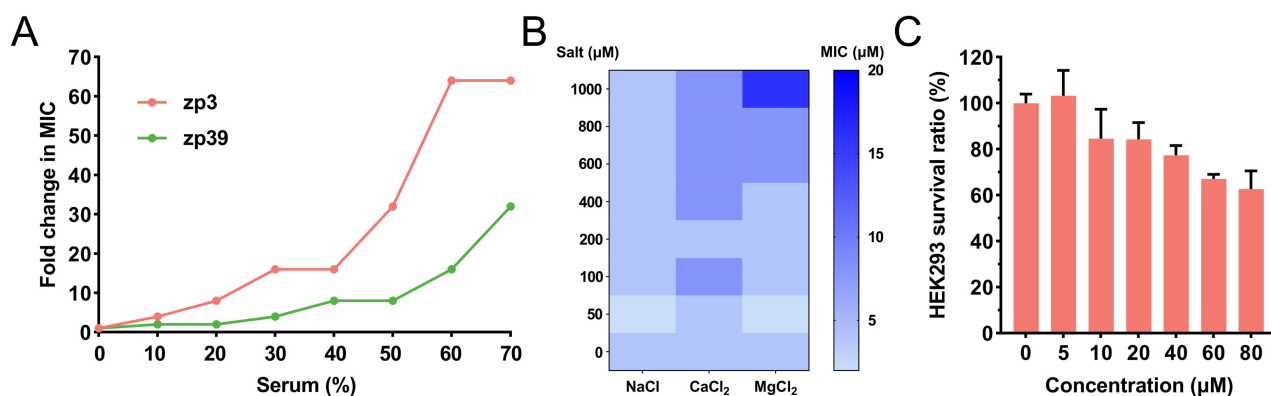


Figure 3. Bioactivities in varied situations and cytotoxicity. (A) Fold change in MIC of zp39 against *E. coli* O157:H7 in the presence of serum; (B) MIC of zp39 against *E. coli* O157:H7 in the presence of extra salts; (C) survival ratio of HEK293 cells after zp39 treatment

HEK293 cells are employed to evaluate the cytotoxicity of zp39 to mammalian cells (Figure 3C). Compared with the control group, HEK293 cells exposed to 80 $\mu\text{mol/L}$ zp39 demonstrated a > 60% survival ratio.

Action mechanisms of zp39

SYTOX Green assay was applied to measure the membrane permeability change after the zp39 treatment (Figure 4A). Higher fluorescence units suggest enhanced cell membrane permeability. In this test, positive peaks at 523 nm (maximum emission wavelength) exhibited a significant dose-dependent effect. Compared with the control group (0 $\mu\text{mol/L}$), membrane permeability of zp39-treated *E. coli* O157:H7 cells increased 1.2-fold (4 $\mu\text{mol/L}$), 1.3-fold (8 $\mu\text{mol/L}$), 1.7-fold (16 $\mu\text{mol/L}$) and 3.0-fold (32 $\mu\text{mol/L}$), respectively.

As indicated by Figure 4B, after merely 10 minutes of treatment by zp39, fluorescence units of *E. coli* O157:H7 membrane potential indicator DiSC₃(5) have increased 1.5-fold (4 $\mu\text{mol/L}$) and 2.5-fold (32 $\mu\text{mol/L}$), showing a statistically significant difference with the PBS-treated group. As a reference, a well-known membrane potential modulator valinomycin (1 $\mu\text{mol/L}$) caused an approximate 2-fold signal increase under the same period.

Cellular morphologies of *E. coli* O157:H7 before and after zp39 treatment were captured by SEM and STEM (Figure 4C). Normally, bacterial cells appeared as plump rod shapes. However, zp39 treatment (32 $\mu\text{mol/L}$, 2 h) could lead to marked cellular shrinkage and deformation. In the STEM image of zp39 treated *E. coli* O157:H7, hollow cells, and even broken cellular fragments can be identified.

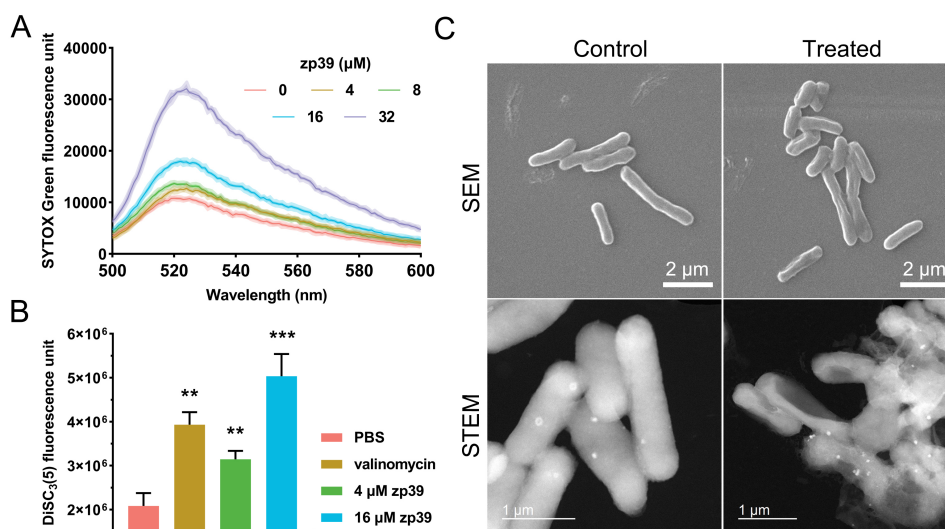


Figure 4. Mechanistic studies. (A) Membrane permeability test; (B) membrane potential test and valinomycin concentration was 1 μmol/L. ** $P < 0.01$, *** $P < 0.001$; (C) SEM and STEM images of *E. coli* O157:H7 before and after zp39 treatment

Controlling EHEC in spinach juice

Next, the antibacterial activity of zp39 in spinach juice was investigated. The results shown in Figure 5A demonstrated that the number of living bacteria had dropped significantly after 16 and 64 μmol/L zp39 treatment in 2 h. On average, the values of log₁₀ CFU/mL were 6.0 (control), 5.7 (4 μmol/L), 5.1 (16 μmol/L), and 4.4 (64 μmol/L), respectively. In other words, > 90% of *E. coli* O157:H7 cells were killed within 2 h in the presence of 64 μmol/L zp39.

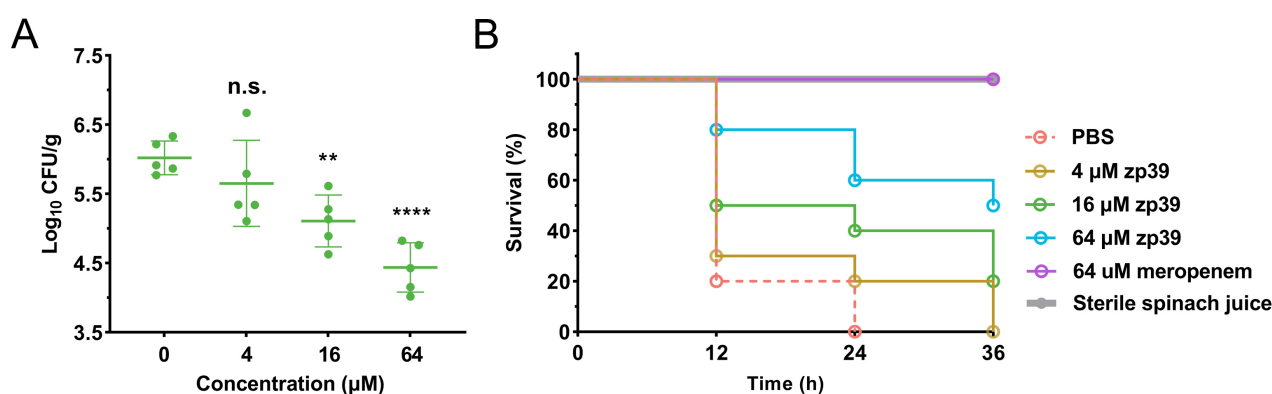


Figure 5. Antibacterial potency of zp39 in spinach juice. (A) Living bacterial colonies in the different treatment groups. ** $P < 0.01$, **** $P < 0.0001$, n.s. means no significant difference; (B) larvae survival ratio in the different treatment groups ($n = 10$ in each group)

Feeding larvae with this contaminated spinach juice, survival curves for each testing group can be summarized (Figure 5B). For negative control which sterile spinach juice was injected, 100% of larvae survived after 36 h of exposure. For positive control, PBS-treated *E. coli* O157:H7-contaminated spinach juice was injected, all larvae died after 24 h of exposure. In the low concentration group (4 μmol/L), the final death time of 20% of larvae extended from 24 h to 36 h after *E. coli* O157:H7 infection. In medium concentration (16 μmol/L) and high concentration (64 μmol/L) groups, 20% and 50% of larvae survived, respectively, after 36 h of exposure.

Discussion

In this work, we first synthesized peptide zp39 and investigated its possible conformation. CD data indicated that a modest amphiphilic environment like a TFE solution was conducive to the formation of the helical structure of zp39. Similar to many cationic amphiphiles [20], zp39 may change its spatial structure

under the induction of the bacterial cell membrane, which could facilitate its binding to the surface of bacteria via electrostatic attraction and hydrophobic affinity.

The growth curve showed that zp39 could significantly reduce the reproduction rate of *E. coli* O157:H7. Subsequent time-kill assay further proved that zp39 worked in a bactericidal mode. LIVE/DEAD staining images hinted that zp39 probably inflicted damage on the membrane of *E. coli* O157:H7 cells because the dye propidium iodide can only bind to DNA through an impaired cell envelope, thus emitting red *E. coli* fluorescence [21].

Due to the incorporation of two dextrorotatory amino acids, zp39 is relatively robust against hydrolysis by proteases comparing with its analog zp3 containing no unnatural residues. Furthermore, the presence of a high concentration of salts had no significant impacts on the antibacterial activity of zp39 against EHEC, particularly attractive for its future application in foods with heavy salts [22]. Cytotoxicity test revealed that zp39 had a great selectivity index of > 20, determined as the half maximal inhibitory concentration to HEK293 cells (> 80 $\mu\text{mol/L}$) to the MIC against *E. coli* O157:H7 (4 $\mu\text{mol/L}$).

Membrane permeability is an important indicator of whether antibacterial molecules can enter the interior of bacteria [23]. Our study illustrated that peptide zp39 was able to augment the permeability of *E. coli* O157:H7, which may seriously hinder the normal physiological function of the cell membrane. Meanwhile, cellular membrane potential was dissipated after zp39 treatment, indicating that the interaction between zp39 and bacterial cell membrane could lead to prompt cationic electrical movement across the phospholipid bilayers. The influence on membrane permeability and potential was adverse to the existence of bacteria [24]. The attack of zp39 also distorted *E. coli* O157:H7 cells. Damaged peripheral structures, dissipation of membrane potential, and possible cytoplasmic leakage collectively contributed to the death of this pathogen.

In many cases, humans get infected by EHEC through the consumption of contaminated food [25]. Fresh-squeezed fruit/vegetable juices and ready-to-eat foods are especially risky because of the lack of high-temperature cooking and other sterilization procedures [26]. Worse still, they often contain a lot of ingredients, including salts and enzymes, which may reduce the bioactivity of antibacterial peptides. Here, we showed that the studied peptide zp39 could resist the influences of such factors and maintained a highly effective bactericidal effect in spinach juice. Its satisfactory stability may be partly due to two unnatural amino acids, dextrorotatory isoleucine, and lysine. *Galleria mellonella* assay also confirmed that zp39-treated *E. coli* O157:H7-contaminated spinach juice showed reduced toxicity to larvae. The improved survival ratio (at medium and high concentration groups) proved that zp39 may be a potential antibacterial agent in precaution of *E. coli* O157:H7-associated infection.

Abbreviations

CD: circular dichroism

CFU: colony forming unit

DiSC₃(5): 3,3'-dipropylthiadicarbocyanine iodide

E. coli: *Escherichia coli*

EHEC: enterohemorrhagic *Escherichia coli*

MHB: Mueller-Hinton broth

MIC: minimal inhibitory concentration

OD₆₀₀: 600 nm optical density

PBS: phosphate buffered saline

SEM: scanning electron microscopy

STEM: scanning transmission electron microscopy

TFE: trifluoroethanol

Declarations

Acknowledgments

We thank the University Research Facilities in Life Sciences (ULS) of The Hong Kong Polytechnic University for providing facilities.

Author contributions

PZ: Conceptualization, Methodology, Investigation, Writing—original draft. XY: Methodology. KYW: Resources, Supervision. SC: Resources, Supervision. KFC: Resources, Supervision. SSYL: Resources, Supervision, Project administration, Funding acquisition. LY: Writing—review & editing, Project administration, Funding acquisition. All authors read and approved the submitted version.

Conflicts of interest

The authors declare that they have no conflicts of interest.

Ethical approval

Not applicable.

Consent to participate

Not applicable.

Consent to publication

Not applicable.

Availability of data and materials

Not applicable.

Funding

This work was supported by the National Natural Science Foundation of China [32102032] and the Health and Medical Research Fund Hong Kong [21200782].

Copyright

© The Author(s) 2023.

References

1. Riley LW. Extraintestinal foodborne pathogens. *Annu Rev Food Sci Technol*. 2020;11:275–94.
2. Mead PS, Griffin PM. *Escherichia coli* O157:H7. *Lancet*. 1998;352:1207–12.
3. Larsen MH, Dalmaso M, Ingmer H, Langsrud S, Malakauskas M, Mader A, et al. Persistence of foodborne pathogens and their control in primary and secondary food production chains. *Food Control*. 2014;44:92–109.
4. Sharapov UM, Wendel AM, Davis JP, Keene WE, Farrar J, Sodha S, et al. Multistate outbreak of *Escherichia coli* O157:H7 infections associated with consumption of fresh spinach: United States, 2006. *J Food Prot*. 2016;79:2024–30.
5. Hassan R, Seelman S, Peralta V, Booth H, Tewell M, Melius B, et al. A multistate outbreak of *E Coli* O157:H7 infections linked to soy nut butter. *Pediatrics*. 2019;144:e20183978.
6. Lazzaro BP, Zasloff M, Rolff J. Antimicrobial peptides: application informed by evolution. *Science*. 2020;368:eaau5480.

7. Zhang H, Chen S. Cyclic peptide drugs approved in the last two decades (2001-2021). *RSC Chem Biol.* 2021;3:18–31.
8. Levine DP. Vancomycin: a history. *Clin Infect Dis.* 2006;42:S5–12.
9. Shin JM, Gwak JW, Kamarajan P, Fenno JC, Rickard AH, Kapila YL. Biomedical applications of nisin. *J Appl Microbiol.* 2016;120:1449–65.
10. Gottler LM, Ramamoorthy A. Structure, membrane orientation, mechanism, and function of pexiganan – a highly potent antimicrobial peptide designed from magainin. *Biochim Biophys Acta.* 2009;1788:1680–6.
11. He Q, Yang Z, Zou Z, Qian M, Wang X, Zhang X, et al. Combating *Escherichia coli* O157:H7 with functionalized chickpea-derived antimicrobial peptides. *Adv Sci.* 2023;10:e2205301.
12. Zeng P, Yi L, Cheng Q, Liu J, Chen S, Chan KF, et al. An ornithine-rich dodecapeptide with improved proteolytic stability selectively kills gram-negative food-borne pathogens and its action mode on *Escherichia coli* O157:H7. *Int J Food Microbiol.* 2021;352:109281.
13. Zeng P, Xu C, Cheng Q, Liu J, Gao W, Yang X, et al. Phenol-soluble-modulin-inspired amphipathic peptides have bactericidal activity against multidrug-resistant bacteria. *ChemMedChem.* 2019;14:1547–59.
14. Scotti R, Casciaro B, Stringaro A, Morgia F, Mangoni ML, Gabbianelli R. Derivatives of esculentin-1 peptides as promising candidates for fighting infections from *Escherichia coli* O157:H7. *Antibiotics.* 2022;11:656.
15. Singh S, Singh H, Tuknait A, Chaudhary K, Singh B, Kumaran S, et al. PEPstrMOD: structure prediction of peptides containing natural, non-natural and modified residues. *Biol Direct.* 2015;10:73.
16. Morrow JA, Segall ML, Lund-Katz S, Phillips MC, Knapp M, Rupp B, et al. Differences in stability among the human apolipoprotein E isoforms determined by the amino-terminal domain. *Biochemistry.* 2000;39:11657–66.
17. Zeng P, Zhang P, Yi L, Wong KY, Chen S, Chan KF, et al. A novel ESKAPE-sensitive peptide with enhanced stability and its application in controlling multiple bacterial contaminations in chilled fresh pork. *Food Chem.* 2023;413:135647.
18. CLSI. Methods for dilution antimicrobial susceptibility tests for bacteria that grow aerobically. Wayne, PA: Clinical and Laboratory Standards Institute; 2006.
19. Te Winkel JD, Gray DA, Seistrup KH, Hamoen LW, Strahl H. Analysis of antimicrobial-triggered membrane depolarization using voltage sensitive dyes. *Front Cell Dev Biol.* 2016;4:29.
20. Ong ZY, Wiradharma N, Yang YY. Strategies employed in the design and optimization of synthetic antimicrobial peptide amphiphiles with enhanced therapeutic potentials. *Adv Drug Deliv Rev.* 2014;78:28–45.
21. Riccardi C, Nicoletti I. Analysis of apoptosis by propidium iodide staining and flow cytometry. *Nat Protoc.* 2006;1:1458–61.
22. Song J, Peng S, Yang J, Zhou F, Suo H. Isolation and identification of novel antibacterial peptides produced by *Lactobacillus fermentum* SHY10 in Chinese pickles. *Food Chem.* 2021;348:129097.
23. Guha S, Ghimire J, Wu E, Wimley WC. Mechanistic landscape of membrane-permeabilizing peptides. *Chem Rev.* 2019;119:6040–85.
24. Zeng P, Cheng Q, Xu J, Xu Q, Xu Y, Gao W, et al. Membrane-disruptive engineered peptide amphiphiles restrain the proliferation of penicillins and cephalosporins resistant *Vibrio alginolyticus* and *Vibrio parahaemolyticus* in instant jellyfish. *Food Control.* 2022;135:108827.
25. Nguyen Y, Sperandio V. Enterohemorrhagic *E. coli* (EHEC) pathogenesis. *Front Cell Infect Microbiol.* 2012;2:90.
26. Moretro T, Langsrud S. Residential bacteria on surfaces in the food industry and their implications for food safety and quality. *Compr Rev Food Sci Food Saf.* 2017;16:1022–41.